



Original article

Synthesis, DNA/RNA affinity and antitumour activity of new aromatic diamidines linked by 3,4-ethylenedioxythiophene

Ivana Stolić^{a,1}, Katarina Mišković^{b,1}, Ivo Piantanida^c, Mirela Baus Lončar^{b,d}, Ljubica Glavaš-Obrovac^{b,e,*}, Miroslav Bajić^{a,**}

^a Department of Chemistry and Biochemistry, Faculty of Veterinary Medicine, University of Zagreb, Heinzelova 55, 10000 Zagreb, Croatia

^b Laboratory of Functional Genomics and Tissue Culture, School of Medicine, J. J. Strossmayer University of Osijek, 31000 Osijek, Croatia

^c Division of Organic Chemistry and Biochemistry, Ruđer Bošković Institute, Zagreb, Croatia

^d Division of Molecular Medicine, Ruđer Bošković Institute, Zagreb, Croatia

^e Clinical Institute of Nuclear Medicine and Rad. Protection, Clinical Hospital Centre Osijek, Osijek, Croatia

ARTICLE INFO

Article history:

Received 23 September 2010

Received in revised form

4 December 2010

Accepted 14 December 2010

Available online 21 December 2010

Keywords:

Diphenylamidine

3,4-Ethylenedioxythiophene

DNA/RNA binding

Antitumour activity

ABSTRACT

A series of novel 2,5-bis(amidinophenyl)-3,4-ethylenedioxythiophenes (**5–10** and **15**) has been synthesized. Compounds **5–10** bind to the DNA minor groove as the dominant binding site and strongly stabilize the double helix of ct-DNA. Surprisingly, the same compounds also thermally stabilize ds-RNA, whereby most of them form stacked dimers along the RNA double helix. The only exception is compound **15** which, due to its structural features, showed no interaction with DNA or RNA. Compounds **5–10** have shown a moderate to strong cytotoxic effect ($GI_{50} = 1.5–9.0 \mu\text{M}$) on a panel of seven tumour cell lines. The diimidazoline derivative **9**, due to its highest inhibitory potential on the growth of all tested tumour cell lines, was investigated in more detail by testing its ability to enter into cells and influence the cell cycle. Compound **9** ($5 \mu\text{M}$) was internalized successfully in cell cytoplasm during a 30-min incubation period, followed by nuclear localization upon 90-min incubation. Significant arrest in HeLa cells in the G2/M phase, shown by cell cycle analysis at an equitoxic ($50 \mu\text{M}$) concentration, suggests interaction of a studied compound with cellular DNA as the main mode of biological action.

© 2010 Elsevier Masson SAS. All rights reserved.

1. Introduction

With the aging of the world's population, changes in dietary habits and the increasing environmental pollution, cancer has emerged as the top threat to human life worldwide [1]. A major goal in the current development of novel chemotherapeutics is to maximize therapeutic responses by increasing their selectivity [2]. One of the approaches is synthesis of small organic molecules with the ability to recognize and bind to specific DNA sequences [3].

The most studied DNA minor groove binders are aromatic diamidines [4–9]. The ability of this class of compounds to interfere with processes vital to cell survival, e.g. replication and transcription, by competing with proteins such as transcription factors and

topoisomerases, has been confirmed by a number of studies performed over the last few decades [10–18].

The amidinium moiety is known to contribute to the DNA binding of small molecules as well as to the recognition of targeted DNA sequences by electrostatic, van der Waals and hydrogen bonding interactions [5,8]. Although DNA binding is clearly involved, not all diamidines are biologically active. For this reason, it is important to understand how small changes in the structure of a novel compound affect its biological activity.

In our search for analogues with improved DNA binding and antitumour activity, we have focused on bisarylamidines, with an extended thiophene core, namely 3,4-ethylenedioxythiophene or benzo[c]thiophenes, as the central linker [10,19]. We presumed that such a structural change could improve affinity and selectivity of novel molecules for specific DNA sequences by increasing their electron-donating capabilities and potential for hydrogen bonding and van der Waals interactions, as it has been shown by studies of Boykin and co-workers [9,20–23].

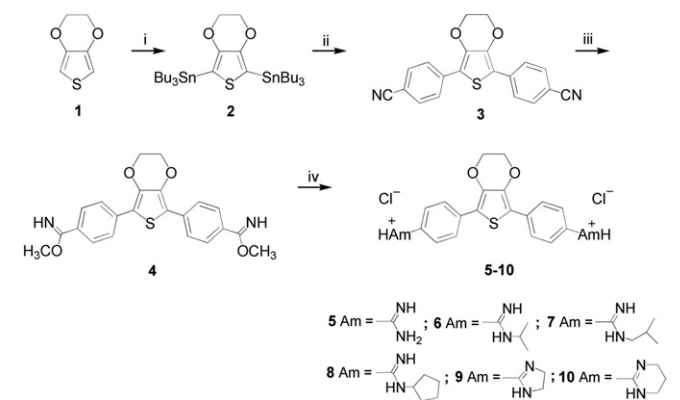
In our previous paper, the effect of 3,4-ethylenedioxy-extension of thiophene core on the DNA/RNA binding properties and biological activity of bisbenzimidazole amidines was described [10].

* Corresponding author. Laboratory of Functional Genomics and Tissue Culture, School of Medicine, J. J. Strossmayer University of Osijek, 31000 Osijek, Croatia. Fax: +385 31 512 227.

** Corresponding author. Tel.: +385 1 2390300; fax: +385 1 2441390.

E-mail addresses: glavas-obrovac.ljubica@kbo.hr (L. Glavaš-Obrovac), mbajic@vef.hr (M. Bajić).

¹ These authors are contributed equally to this work.



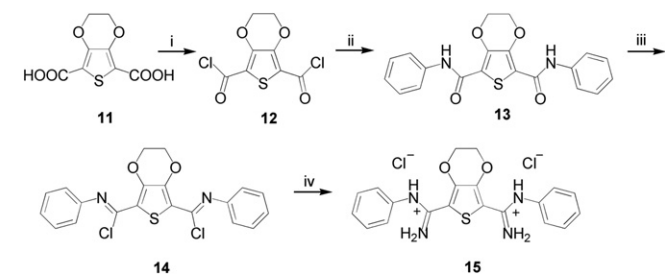
Scheme 1. Reagents: (i) 1. *n*-BuLi, THF, 2. Bu₃SnCl; (ii) Pd(PPh₃)₄, 4-bromobenzonitrile, THF; (iii) HCl(g)/methanol, dioxane; (iv) 1. R₁-NH₂, methanol, 2. HCl(g)/ethanol.

In this series of compounds, the most promising biological activity was shown by the alkyl substituted amidine derivative. Following these results, we report here the synthesis, DNA/RNA binding properties and antitumour activities of 2,5-bis(4-amidinophenyl)-3,4-ethylenedioxythiophene derivatives with alkyl substituted or cyclic amidine at terminal positions. In addition, we have also synthesized compound **15** with amidino moieties attached directly to 2- and 5-positions of 3,4-ethylenedioxythiophene linker and phenyl at terminal positions to compare the impact of the amidine moiety position on DNA affinity and biological properties.

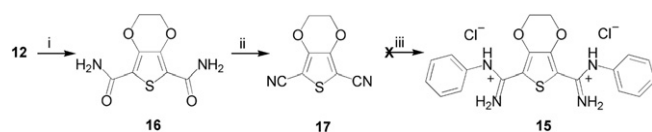
2. Results and discussion

2.1. Chemistry

Scheme 1 depicts the multi-step synthesis used to obtain diimidines **5–10**. The method generally followed the established route [24], involving the preparation of dinitrile and its subsequent conversion into diamidines. The key intermediate, 2,5-bis(4-cyanophenyl)-3,4-ethylenedioxythiophene (**3**), was prepared in two steps starting from 3,4-ethylenedioxythiophene (**1**). The first step involved lithiation of compound **1** with *n*-butyllithium in THF at room temperature, followed by addition of tributyltin chloride to give the corresponding organotin derivative **2**. In the second step, a Stille cross-coupling reaction between compound **2** and 4-bromobenzonitrile, using a catalytic amount of tetrakis(triphenylphosphine) palladium, yielded dinitrile **3**. The latter was transformed, by treatment with methanolic HCl in dioxane, into the corresponding bisimidate ester **4**, which was used directly without further purification and characterization to make the amidines. The dicationic amidine derivatives **5–10** were obtained by reaction of an imidate ester with appropriate amines or diamines in methanol.



Scheme 2. Reagents: (i) SOCl₂, DMF, benzene; (ii) aniline, chloroform; (iii) SOCl₂, DMF, chloroform; (iv) 1. NH₃, chloroform, 2. HCl(g)/ethanol.



Scheme 3. Reagents: (i) NH₄OH, chloroform; (ii) POCl₃, DMF, Py; (iii) 1. HCl(g)/methanol, 2. R-NH₂, methanol.

2,5-Bis(*N*-phenylamidine)-3,4-ethylenedioxythiophene dihydrochloride (**15**) was prepared from dicarboxylic acid (**11**) [25] as outlined in **Scheme 2**. An attempt to synthesize bis(*N*-phenylamidine) at the 2- and 5-positions on the thiophene ring, employing the Pinner reaction from 3,4-ethylenedioxythiophene-2,5-dinitrile (**17**), failed (**Scheme 3**), so an alternative way of synthesis was employed. Diacid **11** was allowed to react with thionyl chloride to give diacid chloride **12**, which was converted by reaction with aniline to the corresponding diacid anilide **13**. Diamide was transformed to diimidine **15** via a two-step process that involved conversion of the former to a diimidoyl chloride derivative using thionyl chloride, followed by reaction with anhydrous ammonia.

2.2. Spectroscopy

In order to study the spectroscopic properties of compounds **5–10** and **15**, their UV–Vis (Fig. 1, Table 1) and fluorescence emission spectra (Fig. 2) were studied. Linear dependence of UV–Vis spectra on the concentration of all the studied compounds in the range c (**5–10**, **15**) = 2.3–5.5 × 10^{−5} mol dm^{−3} suggested the absence of intermolecular interactions between two or more molecules of any of the compounds. Furthermore, the UV–Vis spectra of **5–10** and **15** revealed negligible temperature dependent changes (25–90 °C) and excellent reproducibility upon cooling to 25 °C. Aqueous solutions of all compounds were stable for at least one month.

Comparison of the UV spectra of prepared compounds indicated that substitution of an alkyl group on the amidino nitrogen of parent compound **5** resulted in a bathochromic shift in the UV–Vis spectrum of **9**. An intriguing hypsochromic shift of the absorption maximum of compound **15** compared to compound **5** can be attributed to the direct attachment of amidine to the thiophene core.

All the studied compounds exhibited characteristic fluorescence emission, with maxima at 455–470 nm. Comparison of fluorescence spectra (Fig. 2) revealed the influence of structure on

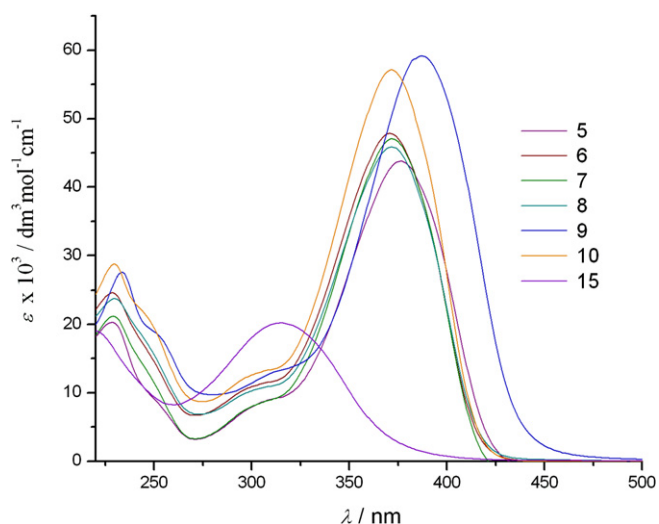


Fig. 1. UV–Vis spectra of **5–10**, and **15** at $c = 2.28\text{--}4.61 \times 10^{-5}$ mol dm^{−3}; pH 7.0, sodium cacodylate/HCl buffer, $l = 0.05$ mol dm^{−3}.

Table 1
Electronic absorption data of **5–10** and **15**.^a

	λ_{\max}/nm	$\epsilon \times 10^3/\text{dm}^3 \text{ mol}^{-1} \text{ cm}^{-1}$
5	376	45.91
6	371	49.35
7	371	47.47
8	372	46.61
9	387	59.66
10	372	57.11
15	315	22.02

^a Sodium cacodylate buffer, pH 7.0, $I = 0.05 \text{ mol dm}^{-3}$.

emission of the compounds. It is interesting to note that alkyl derivatives **6** and **7** exhibited stronger fluorescence than cyclopentyl derivate **8** and cyclic analogues **9** and **10** compared to parent compound **5**. These data show a pronounced impact of electronic properties of the studied molecules on fluorescence emission.

2.3. Interactions with double stranded (ds-) DNA and RNA

2.3.1. UV–Vis titrations with double stranded DNA

The UV–Vis spectra of the studied compounds exhibited strong hypochromic and bathochromic changes upon addition of *calix* thymus (ct)-DNA under the conditions of an excess of compound over DNA base pairs (ratio $r_{[\text{compound}]/[\text{ct-DNA}]}$ > 0.5 for **5** and **9**; $r = 0.4$ for **6**; $r = 0.2$ for **7**, **8** and **10**), while further additions of ct-DNA (excess of DNA base pairs over compound; $r \ll 0.2$) resulted in a hyperchromic effect and additional bathochromic shift of maxima in the UV–Vis spectra (Fig. 3). Thus, the final (at high excess of ct-DNA; $r_{[\text{compound}]/[\text{ct-DNA}]} = 0.02$) bathochromic shifts of the absorption maxima of **5–10** at $\lambda_{\max} > 300 \text{ nm}$ were between +16 and +25 nm. The observed changes in **5–10**/ct-DNA titrations, along with a clear deviation from the isobestic points, supported formation of at least two different types of complexes with ct-DNA. Surprisingly, addition of ct-DNA did not yield any measurable changes in the UV–Vis spectrum of **15**.

2.3.2. Fluorimetric titrations with ct-DNA

Addition of ct-DNA led to a high increase of fluorescence emission of compounds **5–10** (Fig. 4). Similarly as observed in UV–Vis titration experiments, titration with ct-DNA resulted in

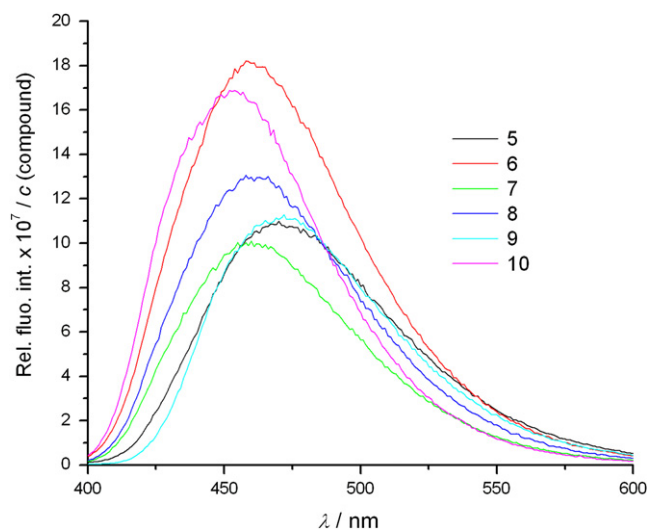


Fig. 2. Fluorescence emission spectra of **5–10** at $c = 3.98\text{--}4.09 \times 10^{-6} \text{ mol dm}^{-3}$; pH 7.0, sodium cacodylate/HCl buffer, $I = 0.05 \text{ mol dm}^{-3}$; at $\lambda_{\text{exc.}} = 376$ (**5**), 371 (**6**, **7**), 372 (**8**, **10**), 387 (**9**) nm.

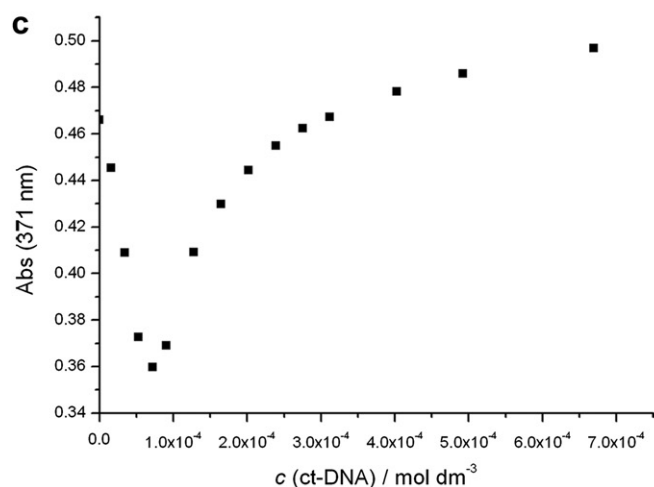
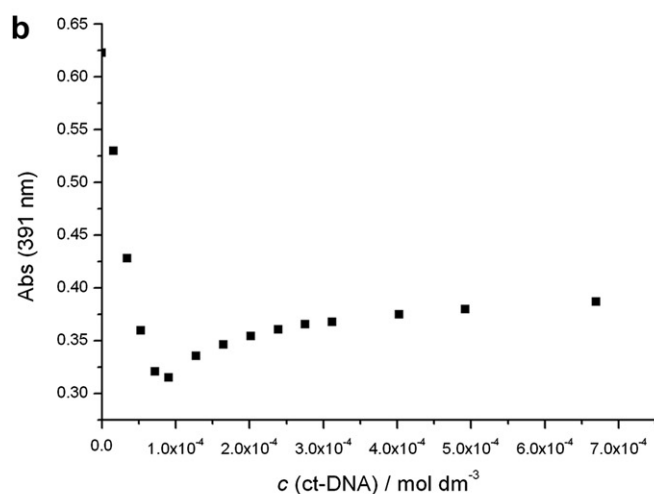
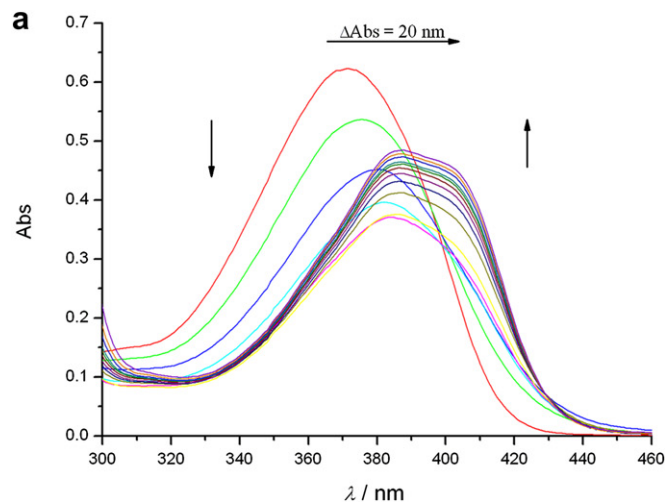


Fig. 3. (a) Changes in UV–Vis spectrum of **7** ($c = 1.97 \times 10^{-5} \text{ mol dm}^{-3}$) upon titration with ct-DNA; Dependence of the absorbance of **7** at $\lambda_{\max} = 391 \text{ nm}$ (b) and 371 nm (c) on $c(\text{ct-DNA})$, at pH 7.0, sodium cacodylate buffer, $I = 0.05 \text{ mol dm}^{-3}$.

opposite changes of fluorescence of compounds **5–10**, where the breakpoint for all titrations was at about the ratio $r_{[\text{compound}]/[\text{ct-DNA}]} = 0.2$. Several different binding modes were present under the conditions of an excess of compound over DNA ($r > 0.2$, fluorescence quenching), including non-specific agglomeration of positively charged small molecules along the negatively charged

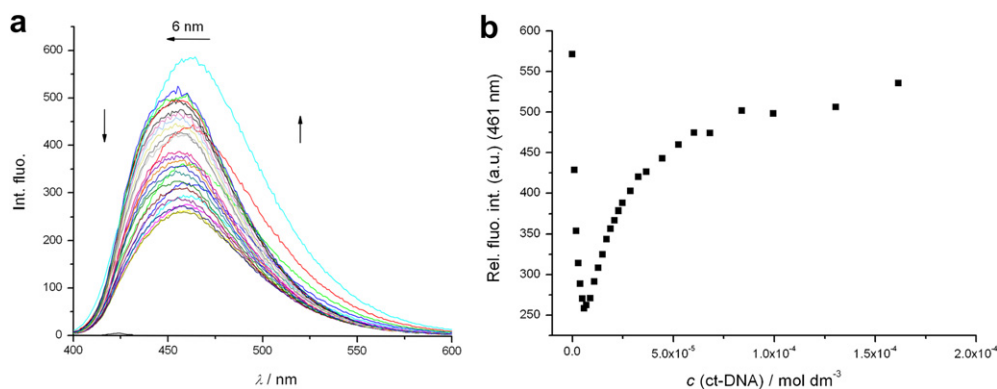


Fig. 4. (a) Changes in the fluorescence spectrum of **7** ($c = 1.0 \times 10^{-6} \text{ mol dm}^{-3}$, $\lambda_{\text{exc}} = 371 \text{ nm}$) upon titration with ct-DNA; (b) Dependence of fluorescence emission of **7** at $\lambda_{\text{max}} = 461 \text{ nm}$ on c (ct-DNA). Done at pH 7.0, sodium cacodylate buffer, $I = 0.05 \text{ mol dm}^{-3}$.

DNA backbone as well as binding into the minor groove of DNA. In contrast, one dominant binding mode prevailed at an excess of DNA over compound ($r \ll 0.2$, fluorescence increase), most likely the mutually independent binding of the studied molecules inside the DNA minor groove. To determine the binding affinity of **5–10** toward ct-DNA, we processed the titration data collected at a large excess of DNA ($r \ll 0.2$, fluorescence increase) by means of the Scatchard equation [26], which yielded comparable binding constants for all compounds ($\log K_s = 5.5\text{--}5.8$ for the Scatchard ratio $n_{[\text{bound compound}]/[\text{ct-DNA}]} = 0.2$).

2.3.3. Circular dichroism titrations

We chose CD spectroscopy as a highly sensitive method to assess conformational changes in the secondary structure of polynucleotides [27] in order to gain more information on the binding mode and the structure of the complexes formed. In addition, achiral small molecules can show induced CD signals (ICD) upon binding to polynucleotides, giving useful information about the modes of interaction [27,28]. The sign and magnitude of the ICD band can depend on the binding geometry. Ligand–ligand stacking is expected to give a strong bisignate exciton CD band. Minor groove binding to ds-DNA orientates the ligand approximately at 45° in respect to the DNA chiral axis, giving a strong positive ICD band. Intercalation brings the aromatic moiety of the ligand in a coplanar arrangement with the base pairs, giving only a weak ICD band (not always but in most cases of a negative sign due to parallel orientation of the transition vector of the ligand and longer axis of the surrounding base pairs) [29,30].

Addition of **5–10** to the ct-DNA resulted in dramatic changes of the corresponding CD spectrum (Fig. 5). Strongly pronounced non-linear dependence of the changes in CD spectra on the ratio $r_{[\text{compound}]/[\text{ct-DNA}]}$ (Fig. 6) suggests saturation of dominant binding sites at about $r = 0.2\text{--}0.4$.

Under the conditions of higher excess of DNA over compounds (ratio $r < 0.3$), addition of compounds **5–10** caused a pronounced decrease of ct-DNA CD band at 285 nm, accompanied by a weak induced (ICD) band at 300–310 nm (agreeing nicely with the shoulder in the corresponding UV–Vis spectra) and a strong ICD band at about 390–400 nm (agreeing nicely with the main maxima in the corresponding UV–Vis spectra). Further additions leading to an excess of compound over DNA (ratio $r > 0.3$) resulted in a further increase of the aforementioned changes in CD spectra for compounds **5–8** and **10**, whereby isoelliptic points were largely retained. Contrary to **5–8** and **10**, an excess of compound **9** over DNA ($r > 0.2$) yielded new ICD bisignate exciton bands characterized by a negative band at $\lambda_{\text{max}} = 370 \text{ nm}$, positive band at $\lambda_{\text{max}} = 410 \text{ nm}$ and isoelliptic point at $\lambda = 385 \text{ nm}$ (agreeing nicely

with the UV–Vis spectrum maximum). Strong positive ICD bands of **5–8** and **10**, as well as of **9** at $r < 0.2$, indicate binding of single molecules within the DNA minor groove as the dominant type of interaction [29]. However, the observed ICD bisignate exciton bands for **9** at $r > 0.2$ strongly support dimer formation of **9**, most likely also within the DNA minor groove [29,31].

Additions of **5–10** to ds-RNA at the ratio $r_{[\text{compound}]/[\text{poly A–poly U}]} < 0.2$ (excess of RNA over compound) in most cases resulted in only a minor decrease of the RNA CD band at $\lambda_{\text{max}} = 265 \text{ nm}$. No induced (ICD) bands were observed at $\lambda > 300 \text{ nm}$, with the exception of the weak positive ICD band of **9** at $\lambda_{\text{max}} = 410 \text{ nm}$. However, further additions of most compounds ($r > 0.2$, excess of compound over RNA) resulted in pronounced ICD bands at $\lambda > 300 \text{ nm}$, with shapes depending on the compound structure. Additions of compounds **5, 8, 9** and **10** resulted in the appearance of bisignate exciton couplets, which suggested formation of stacked dimers uniformly oriented in respect to the ds-RNA chiral axis [27,29], most likely bound within the hydrophobic and narrow major groove of the RNA α -helix [32]. At variance with other compounds, compound **6** yielded only a weak negative ICD band at $\lambda_{\text{max}} = 370 \text{ nm}$, suggesting interactions of single molecules with RNA. Only compounds **7** and **15** produced no ICD bands under any conditions.

It is noteworthy that **15** did not exhibit any significant change in CD spectra of either ds-DNA or ds-RNA.

2.3.4. Thermal denaturation experiments

Interactions of compounds **5–10** and **15** with ct-DNA and with double stranded RNA (poly A–poly U) were studied by thermal denaturation experiments (Table 2). Addition of **5–10** strongly stabilized the double helix of ct-DNA, whereby the non-linear dependence of ΔT_m values obtained for ct-DNA/**5–10** on ratio r suggested saturation of binding sites at about $r = 0.2\text{--}0.3$. The obtained ΔT_m values were comparable, indicating minor impact of the structure of **5–10** on the stabilization of ct-DNA. Intriguingly, the studied compounds exerted quite a different effect on thermal denaturation of ds-RNA (poly A–poly U). Comparison of ΔT_m values obtained for **5–8** revealed that **5**, characterized by non-substituted amidine, had the strongest effect on poly A–poly U stabilization, while systematic increase of the bulkiness of aliphatic substituents on amidine groups in **6–8** series proportionally decreased the thermal stabilization effect. Compounds **9** and **10** characterized by cyclic amidine groups stabilized ds-RNA much more strongly compared to **6–8**. Moreover, compound **9** stabilized similarly ds-DNA and ds-RNA.

These results are in good agreement with the data published by Wilson and co-workers for diphenylfuran diamidines [33,34]. Compounds **5, 9** and **10** had a stronger stabilization effect on the RNA duplex than analogous amidine derivatives from the

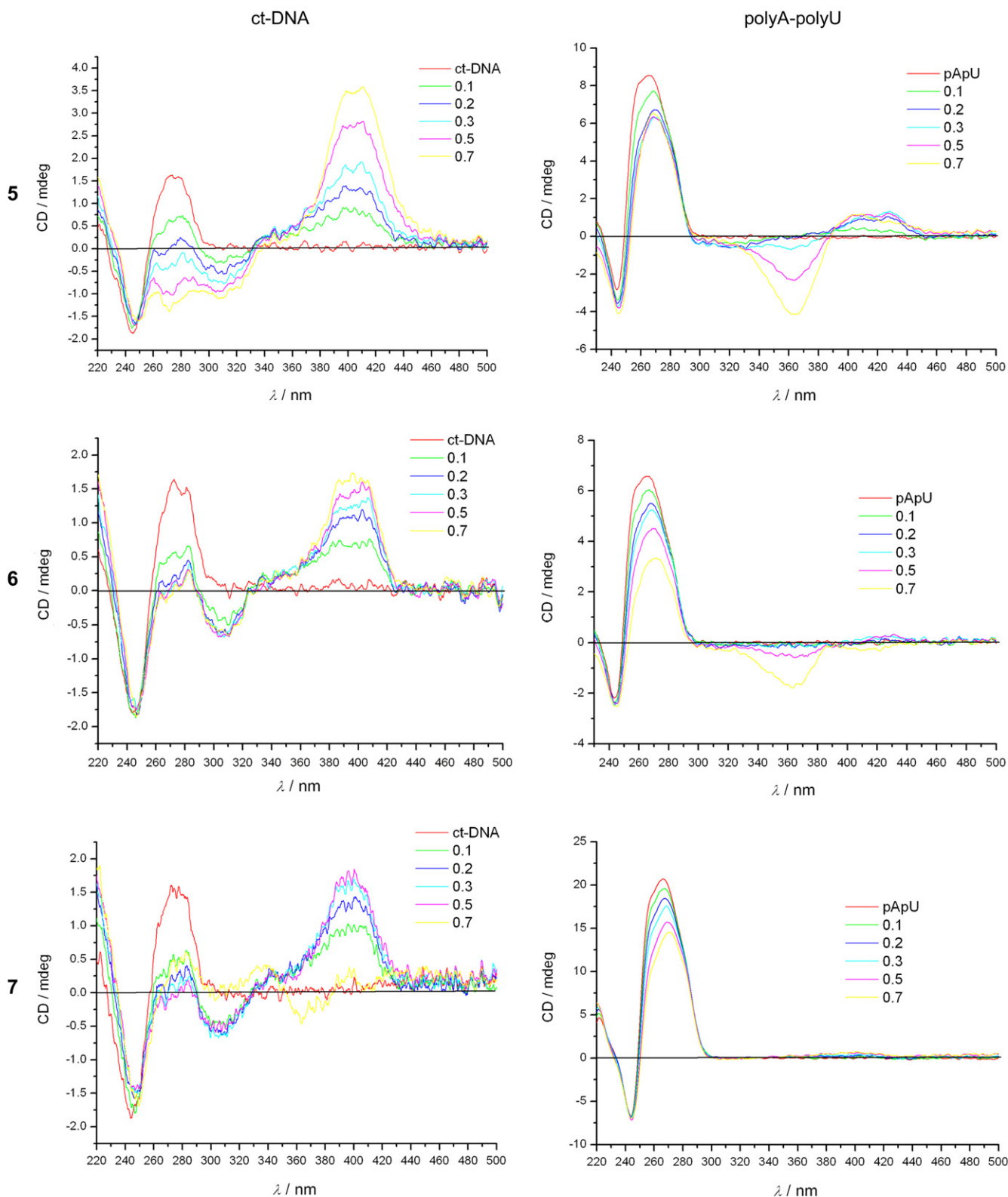


Fig. 5. CD titration of polynucleotides ($c = 2.0 \times 10^{-5} \text{ mol dm}^{-3}$) with **5–10** at molar ratios $r = [\text{compound}]/[\text{polynucleotide}]$ (pH 7.0, buffer sodium cacodylate, $l = 0.05 \text{ mol dm}^{-3}$).

diphenylfuran series. A possible reason for stronger stabilization could be 3,4-ethylenedioxy extension of the central core, which increased hydrophobicity compared to the previously studied furan analogues. The strongest binding effect of the imidazoline derivative **9** could be explained by formation of an intercalation

complex with polyA–polyU at an excess of RNA over compound ($r < 0.3$) [33].

Addition of **15** did not affect denaturation of ct-DNA and ds-RNA, which is in accord with the lack of any interaction in UV–Vis and fluorimetric titrations.

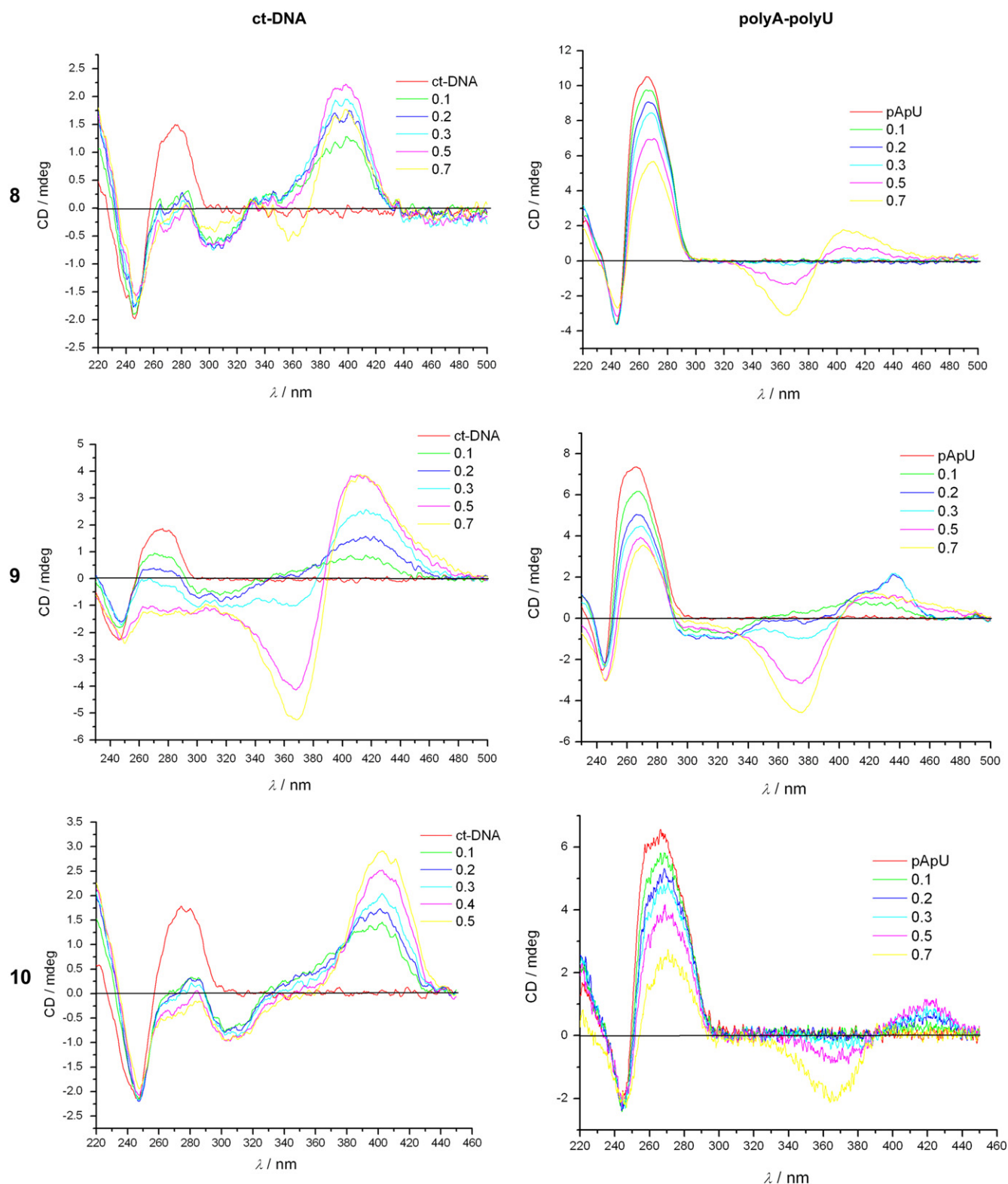


Fig. 5. (continued).

2.3.5. Ethidium bromide displacement experiments

The binding constants and Scatchard ratios n could be calculated only at a high excess of DNA due to mixed binding modes of the studied compounds close to saturation of the binding site of ds-DNA. We performed the ethidium bromide

(EB) displacement assay (Fig. 7) as an alternative method to estimate affinity under the conditions of binding site saturation, at least to compare the ability of the studied molecules to compete for binding with a classical intercalator already bound to DNA.

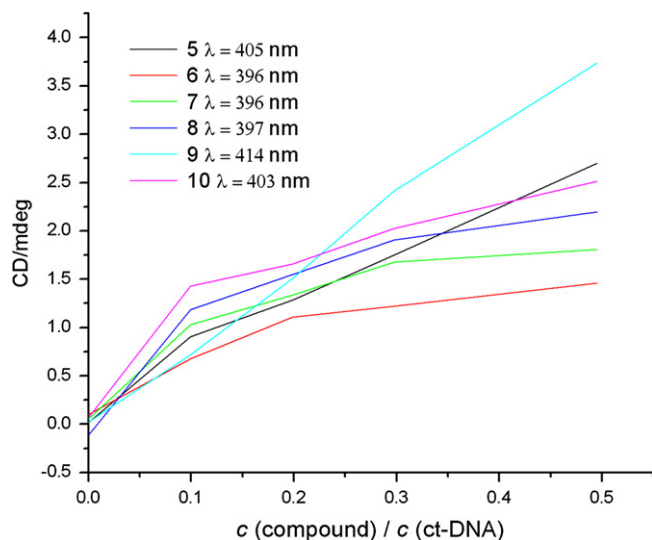


Fig. 6. Induced CD signals of 5–10 plotted against ligand/ct-DNA ratios.

The obtained IC_{50} values (Fig. 7) suggest that affinity of 5–10 toward ct-DNA is comparable to EB affinity. This finding is in good agreement with calculated binding constants, taking into account that the binding constant of EB toward ct-DNA under the same experimental conditions is $\log K_s = 6$ [35].

2.4. Biological results

In the present study, we investigated the cytotoxic properties of newly synthesized compounds 5–10 and 15 and Hoechst 33258 on a panel of seven tumour cell lines of different histological origin and Madine–Darby canine kidney (MDCK) normal cells. The results are presented as the GI_{50} value, a concentration eliciting inhibition of cell growth by 50%. The compounds displayed different growth inhibitory effects in dependence on the dose applied (Table 3) on the 3rd day of incubation. Compound 9 showed a significant potent antitumour effect on tested tumour cells with the GI_{50} value from 1.5×10^{-6} to 9.0×10^{-6} mol dm $^{-3}$ as well as on normal MDCK cells (17.0×10^{-6} mol dm $^{-3}$). All cell lines, except MCF-7, exposed to Hoechst 33258 exhibited GI_{50} from 84×10^{-6} to 191.5×10^{-6} mol dm $^{-3}$. Among the most sensitive cells were MCF-7 cells ($GI_{50} = 2.7 \times 10^{-6}$ mol dm $^{-3}$) and HeLa cells ($GI_{50} = 1.5 \times 10^{-6}$ mol dm $^{-3}$) treated with compound 9. A possible reason for the obtained improved sensitivity of HeLa and MCF-7 cells could be higher cellular uptake in combination

Table 2

The ΔT_m^a values ($^{\circ}C$) of ct-DNA and poly A–poly U upon addition of different ratios r^b of 5–10 and 15 at pH 7.0 (buffer sodium cacodylate, $I = 0.05$ mol dm $^{-3}$).

$r^b =$	ct-DNA			poly A–poly U
	0.1	0.2	0.3	0.3
5	12.2	>16 ^c	>16 ^c	12.6
6	8.4	11.1	12.3	5.8
7	9.0	9.0	15.0	5.2
8	12.3	15.2	>16 ^c	1.4
9	10.8	14.3	>16 ^c	17.0
10	11.8	>16 ^c	>16 ^c	8.2
15	–	–	0	0

^a Error in ΔT_m : ± 0.5 $^{\circ}C$.

^b $r = [\text{compound}]/[\text{polynucleotide}]$.

^c ΔT_m impossible to calculate since T_m is over 100 $^{\circ}C$.

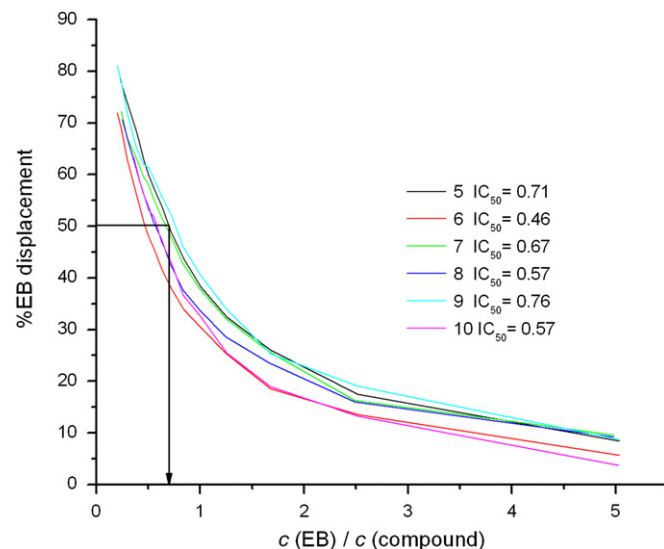


Fig. 7. Ethidium bromide (EB) displacement assay: to ct-DNA solution ($c = 5 \times 10^{-5}$ mol dm $^{-3}$), ethidium bromide ($c = 5 \times 10^{-6}$ mol dm $^{-3}$) was added ($r[\text{EB}]/[\text{ct-DNA}] = 0.1$), and quenching of the EB/DNA complex fluorescence emission ($\lambda_{\text{ex}} = 480$ nm, $\lambda_{\text{em}} = 600$ nm) was monitored as a function of $c(\text{EB})/c(\text{compound})$. The given IC_{50} values represent the ratio $c(\text{EB})/c(\text{compound}) = [\text{Int}(\text{EB}/\text{DNA}) - \text{Int}(\text{EB}_{\text{free}})]/2$, where $\text{Int}(\text{EB}/\text{DNA})$ is fluorescence intensity of the EB/DNA complex and $\text{Int}(\text{EB}_{\text{free}})$ is fluorescence intensity of the free ethidium bromide before DNA is added.

with the dose applied and chemical structure of compound 9. High sensitivity of the HEP-2 cells treated with compound 5 (9.3×10^{-6} mol dm $^{-3}$), compound 6 (9.0×10^{-6} mol dm $^{-3}$), and compound 7 (9.9×10^{-6} mol dm $^{-3}$), respectively, was also observed. The growth of MiaPaCa2 cells treated with 7 was more sluggish ($GI_{50} = 4.9 \times 10^{-6}$ mol dm $^{-3}$) compared to the growth of cells treated with compound 9 (9.0×10^{-6} mol dm $^{-3}$). MDCK line was most sensitive to compound 5 (7.1×10^{-6} mol dm $^{-3}$), while the inhibitory effects of other tested compounds were significantly lower (Table 3). Compound 15 exhibited negligible inhibitory potential against the tumour cell lines tested. TGI (total growth inhibition) values for all compounds on all tested cell lines were higher than 1×10^{-4} mol dm $^{-3}$.

As the chemical structure of compounds is a key determinant of their uptake and allocation in live cells [10], we investigated the cellular uptake of compounds 7, 8 and 9. We used Hoechst 33258 as a reference compound since its nucleus localization is well documented [36]. As expected, after 30 min of incubation, Hoechst 33258, applied at a concentration of 1×10^{-4} mol dm $^{-3}$, was observed in the nucleus of HeLa cells (Fig. 8a). Under the same experimental conditions, compound 9 (5×10^{-6} mol dm $^{-3}$) penetrated into the cell cytoplasm (Fig. 8b) after 30 min of incubation and 60 min later, 9 was localized in the cell nucleus (Fig. 8c). Compared to compound 9, compounds 7 and 8 at 1×10^{-4} mol dm $^{-3}$ concentration slowly entered into the cells. After 2 h of incubation, they were localized in the cytoplasm and nucleus of MiaPaCa2 cells (Fig. 9a and b). Our results indicate that the differences in chemical structure between investigated compounds led to different rates of their entry into cells and intracellular localization.

Cell cycle coordination, according to signals coming from their environment is a fundamental property of cells [37]. One of the hallmarks of carcinogenesis is deregulation of the cell cycle [1]. Some antitumour agents are capable of inducing checkpoint arrest and apoptotic cell death by inducing DNA damage [38–40]. Numerous novel therapeutics affect cells in a specific phase of the cell cycle [41]. Recent evidence implicates DNA repair and the so-called genome integrity checkpoints as culprits whose defects are

Table 3
Cytotoxic activity of tested compounds.

GI ₅₀ (1 × 10 ⁻⁶ mol dm ⁻³) ^a								
Compound	5	6	7	8	9	10	15	Hoechst
<i>Tumour cells</i>								
MCF-7	25.0 ± 15.6	67.5 ± 27.6	7.3 ± 0.8	7.8 ± 1.2	2.7 ± 1.7	8.4 ± 1.2	129.0 ± 18.4	5.7 ± 4.5
NCI-H358	33.0 ± 12.7	112.7 ± 9.5	73.3 ± 2.9	62.2 ± 6.3	4.1 ± 1.0	98.7 ± 10.0	112.0 ± 8.5	91.7 ± 18
CaCo-2	13.0 ± 4.2	76.5 ± 14.8	42.8 ± 29.9	41.0 ± 26.9	3.1 ± 1.3	101.3 ± 15.1	134.0 ± 11.3	84.0 ± 9.8
HEp-2	9.3 ± 1.2	9.0 ± 0	9.9 ± 0.6	61.3 ± 19.9	3.0 ± 0.8	97.7 ± 18.1	100.3 ± 17	132.5 ± 7.8
HeLa	32.3 ± 12.4	72.3 ± 13.3	18.8 ± 9.1	26.7 ± 11.2	1.5 ± 0.8	97.5 ± 10.6	138.5 ± 3.5	115.7 ± 25.5
AGS	116.5 ± 34.6	72.3 ± 18.4	59.3 ± 3.8	45.0 ± 2.6	4.3 ± 3.8	81.7 ± 12.6	113.5 ± 4.9	112.0 ± 12.7
MiaPaCa2	9.3 ± 1.5	13.0 ± 3.5	4.9 ± 7.0	10.9 ± 5.7	9.0 ± 0.9	64.7 ± 25.8	128.5 ± 21.9	191.5 ± 17.7
<i>Normal cells</i>								
MDCK	7.1 ± 1.6	65.3 ± 4.0	59.7 ± 4.2	50.0 ± 5.9	17.0 ± 0.9	82.0 ± 17.7	79.5 ± 17.7	157.5 ± 20.5

Abbreviation (used cell lines): breast adenocarcinoma (MCF-7), bronchioalveolar carcinoma (NCI-H358), colon adenocarcinoma (CaCo-2), larynx carcinoma (HEp-2), cervix adenocarcinoma (HeLa), gastric adenocarcinoma (AGS), pancreatic carcinoma (MiaPaCa) and Madine-Darby canine kidney (MDCK).

Bold values emphasized significant difference in cytotoxic efficiency of investigated compounds on tumour cells compared to normal cells.

^a GI₅₀ value—concentration eliciting inhibition of cell growth by 50%. Data represent the mean GI₅₀ value of three independent experiments ± SD. Cytotoxic activity was analyzed by the MTT assay.

largely responsible for the enhanced genetic instability of tumour cells [42]. The G2/M checkpoint prevents a DNA damaged cell from entering mitosis and gives more time to various repair mechanisms to repair the damage, if possible, or directs the cell into programmed cell death. For this reason, the G2/M checkpoint is of particular interest for novel drug design in the development of antitumour therapy [43].

To elucidate the mechanism of cytotoxic action of compound **9**, its effect on the cell cycle of HeLa cells was monitored. Compound **9**, applied at a concentration of 5 × 10⁻⁵ mol dm⁻³, significantly affected the cell cycle of HeLa cells during monitored incubation periods (24–72 h). Accumulation of cells in the G2/M phase started 24 h after application and increased up to 3 fold over incubation time. Percentage of cells in the G2/M phase slowly increased from

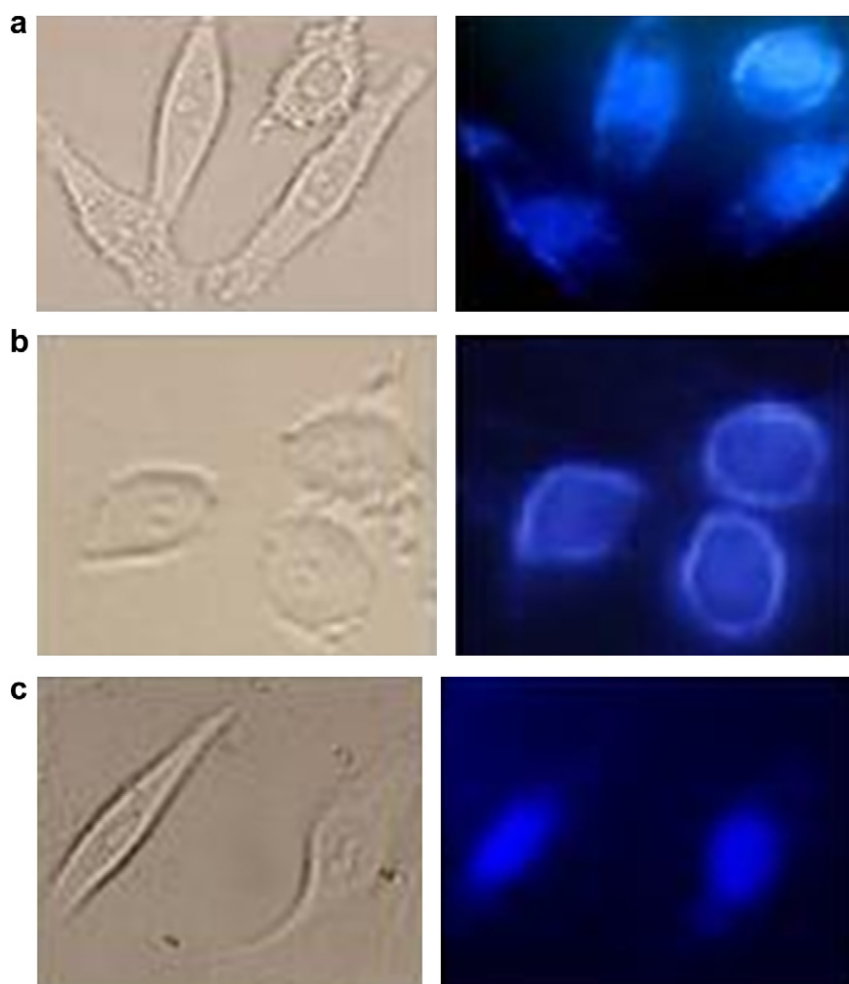


Fig. 8. Fluorescence microscopy analysis of the entry and intracellular distribution of 1 × 10⁻⁴ mol dm⁻³ Hoechst 33258 (a), 5 × 10⁻⁶ mol dm⁻³ compound **9** (b) in HeLa cells after 30 min of incubation, and 5 × 10⁻⁶ mol dm⁻³ compound **9** (c) after 90 min of incubation using BP 450–490 filters, LP 520. Magnification: 400×.

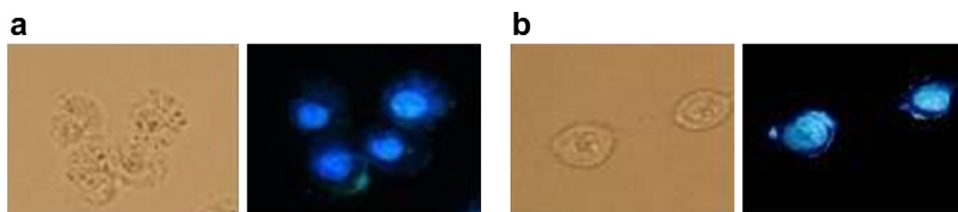


Fig. 9. Fluorescence microscopy analysis of the entry and intracellular distribution of 1×10^{-4} mol dm $^{-3}$ compound **7** (a) and 1×10^{-4} mol dm $^{-3}$ compound **8** (b) in MiaPaCa2 cells after 2 h of incubation using filters BP 450–490, LP 520. Magnification: 400 \times .

17.58% after 24 h to 21.07% after 72 h of treatment, indicating cessation of the cell cycle in that phase. The share of G0/G1, at the same time, decreased to a statistically significant level (Table 4). The observed increase of the G2/M phase arrested cells during prolonged incubation time points to DNA damage as a consequence of compound **9** interaction with intracellular genomic components. Weakened G2/M checkpoint in the therapeutic setting may trigger cell death via mitotic catastrophe. Under the same experimental conditions, Hoechst 33258, used as a binder reference compound, stopped the cell cycle in S phase and G0/G1. The difference between the G1 share of cells treated with compound **9** and Hoechst 33258 at 5×10^{-5} mol dm $^{-3}$ was very small, but statistically important in comparison with control cells.

3. Conclusions

The majority of studied compounds bind strongly to both ds-DNA and ds-RNA. The only exception is compound **15**; comparison of its structure with structures of other compounds clearly shows that the shortening and rigidification of the core by direct attachment of amidines to thiophene hamper its effective interactions with DNA/RNA. Its weak cytotoxic potential for tumour as well as normal epithelial cells has been also confirmed. Furthermore, all applied methods suggest the DNA minor groove as the dominant binding site of **5–10**, where at an excess of DNA single molecules are bound, while at an excess of **5, 8, 9** and **10** they form stacked dimers, most likely also within the DNA minor groove. Surprisingly, compounds **5–10** also thermally stabilize ds-RNA, which is not common for typical DNA minor groove binders, and most of them, when present in excess over RNA, form stacked dimers along the RNA double helix, most likely within the hydrophobic and narrow major groove. However, intercalation of **9** at higher excess of RNA cannot be excluded. An exception is compound **7**, whose molecules seem to moderately stabilize ds-RNA by more or less random binding along the polynucleotide helix, thus lacking any ICD signal. Although compounds **5–10** showed a similar binding potential to the minor groove of ds-DNA and ds-RNA under *in vitro* conditions, they displayed different cytotoxic activity against tumour and normal cells. Cytotoxic effect of compound **9** on tumour cells is in good agreement with the

strength of the observed interactions with DNA and RNA. Its successful entering into the cell cytoplasm and nucleus has been also confirmed. In addition, an increase of the G2/M phase arrested cells treated with compound **9** points to the mitotic cell death as a consequence of its interaction with intracellular genomic components.

4. Experimental

4.1. Synthesis

Solvents were distilled from appropriate drying agents shortly before use. TLC was carried out on DC-plastikfolien Kieselgel 60 F254, Merck. Melting points were determined on a Büchi 510 melting point apparatus and were uncorrected. IR spectra [ν_{\max} /cm $^{-1}$] were obtained on a Bruker Vertex 70 spectrophotometer. The ^1H and ^{13}C NMR spectra were recorded on a Bruker Avance 300 MHz spectrometer. Chemical shifts (δ /ppm) are referred to TMS. Mass spectra were recorded on a Waters Micromass Q-ToF micro. Elemental analyses were performed by the Applied Laboratory Research Department of Ina, d.d., Research and Development Sector, Central Analytical Laboratory. All compounds gave C, H, N and S analyses within $\pm 0.4\%$ of the theoretical values.

4.1.1. 2,5-Bis(4-cyanophenyl)-3,4-ethylenedioxythiophene (**3**)

To a stirred solution of 3,4-ethylenedioxythiophene (6.60 g, 0.046 mol) in freshly distilled THF (230 mL) under a nitrogen atmosphere, 2.5 M *n*-BuLi in hexane (40 mL, 0.1 mol) was slowly added. The resulting solution was stirred for 1 h at room temperature (RT) and 1 h at 75 °C. The mixture was cooled to RT and Bu_3SnCl (26 mL, 31.2 g, 0.096 mol) was added dropwise. The vigorously stirred mixture was refluxed for 21 h. The solvent was removed under reduced pressure, the residue was suspended in anhydrous hexane and the suspension was filtered off. The filtrate was concentrated to dryness under reduced pressure and the obtained solid was dissolved in freshly distilled THF (300 mL) under a nitrogen atmosphere. 4-Bromobenzonitrile (17.76 g, 0.1032 mol) and $[\text{Pd}(\text{PPh}_3)_4]$ (5.126 g, 0.0094 mol) were added to the solution. The vigorously stirred mixture was refluxed for 8 days under a nitrogen atmosphere. The solvent was partially evaporated, dry

Table 4
Effect of compound **9** and Hoechst 33258 on cell cycle progression.^a

Treatment	Phases of cell cycle								
	G0/G1			S			G2/M		
	24 h	48 h	72 h	24 h	48 h	72 h	24 h	48 h	72 h
Control	62.2 \pm 4.4	61.2 \pm 2.3	63.4 \pm 3.2	27.7 \pm 4.2	30.4 \pm 3.7	28.8 \pm 3.2	10.1 \pm 3.4	8.4 \pm 3.9	7.8 \pm 3.1
9 (5×10^{-6} M)	53.3 \pm 6.7*	44.2 \pm 7.2*	46.4 \pm 6.1*	29.1 \pm 7.0	37.3 \pm 10.8	32.5 \pm 10.2	17.6 \pm 4.5*	18.5 \pm 6.8*	21.1 \pm 6.3*
9 (1×10^{-6} M)	55.4 \pm 7.7	59.6 \pm 3.5	62.2 \pm 3.2	30.2 \pm 2.7	33.1 \pm 2.0	25.9 \pm 4.6	14.4 \pm 6.1	7.3 \pm 2.5	11.9 \pm 4.7
Hoechst 33258 (5×10^{-5} M)	51.3 \pm 1.3*	49.0 \pm 4.9*	45.7 \pm 4.5*	41.6 \pm 3.5*	42.6 \pm 3.8*	43.1 \pm 7.9*	7.1 \pm 3.1	8.4 \pm 3.5	11.2 \pm 6.8

^a Data are presented as mean value \pm standard deviation (SD). Statistically significant differences are marked with (*) and set at $p < 0.05$. Experiment was performed three times in two replicates ($n = 6$).

diethyl ether was added and the precipitate was filtered off and recrystallized from CHCl_3 to yield 6.5 g (41.7%) of yellow powder, mp > 250 °C; IR (KBr) $\nu_{\text{max}}/\text{cm}^{-1}$: 3403, 2926, 2223, 1601, 1521, 1483, 1446, 1409, 1374, 1087, 841, 575; ^1H NMR (CDCl_3) δ/ppm : 7.87 (d, 4H, $J = 8.80$ Hz, ArH), 7.68 (d, 4H, $J = 8.78$ Hz, ArH), 4.45 (s, 4H, $\text{OCH}_2\text{CH}_2\text{O}$); ^{13}C NMR ($\text{DMSO}-d_6$) δ/ppm : 141.5, 136.9, 133.4, 126.4, 119.3, 114.8, 109.4, 65.3; Anal. calcd. for $\text{C}_{20}\text{H}_{12}\text{N}_2\text{O}_2\text{S}$ ($M_r = 344.39$): C 69.75, H 3.51, N 8.13, S 9.31; found: C 70.03, H 3.80, N 8.28, S 9.19.

4.1.2. 2,5-Bis(4-amidinophenyl)-3,4-ethylenedioxythiophene dihydrochloride (5)

Dinitrile **3** (0.513 g, 1.5 mmol) was suspended in a mixture of anhydrous methanol (12 mL) and dry dioxane (30 mL), cooled in an ice bath and saturated with dry HCl gas. The suspension was stirred at RT until IR spectra indicated the absence of the cyano peak (3 days). Anhydrous diethyl ether was added to the suspension and the obtained solid was collected by filtration, washed with anhydrous diethyl ether and dried under vacuum to yield 0.668 g (92.5%) of bis(imidate ester hydrochloride) **4**. The resulting salt was used in the next step without any additional purification.

Crude imidate ester **4** (0.668 g, 1.37 mmol) was suspended in anhydrous methanol (80 mL) and the solution was saturated with dry NH_3 gas at ice bath temperature. The flask was sealed, and the suspension was stirred at room temperature for 2 days. The solvent was removed under reduced pressure and the residue was suspended in anhydrous ethanol saturated with HCl(g) and stirred at room temperature for 2 h. The reaction mixture was concentrated and precipitated with dry diethyl ether, the solid was collected by filtration and dried under vacuum at 80 °C for 24 h. Yield: 0.115 g (18.3%) of pale yellow powder, mp > 250 °C; IR $\nu_{\text{max}}/\text{cm}^{-1}$: 3407, 1660, 1602, 1458, 1391, 1089, 924, 850, 753, 689; ^1H NMR ($\text{DMSO}-d_6$) δ/ppm : 9.31 (s, 4H, NH_2), 9.07 (s, 4H, NH_2), 7.94 (d, 4H, $J = 8.95$ Hz, ArH), 7.90 (d, 4H, $J = 8.83$ Hz, ArH), 4.51 (s, 4H, $\text{OCH}_2\text{CH}_2\text{O}$); ^{13}C NMR ($\text{DMSO}-d_6$) δ/ppm : 164.8, 140.9, 137.1, 128.9, 125.8, 125.4, 114.3, 64.8; HRMS: calcd. for $\text{C}_{20}\text{H}_{19}\text{N}_4\text{O}_2\text{S}$ ($M + 1$)⁺, 379.1229; found: 379.1215. Anal. calcd. for $\text{C}_{20}\text{H}_{18}\text{N}_4\text{O}_2\text{S} \cdot 2\text{HCl} \cdot 0.5\text{H}_2\text{O}$ ($M_r = 460.38$): C 52.18, H 4.60, N 12.17, S 6.97; found: C 52.23, H 4.64, N 11.83, S 6.86.

4.1.3. 2,5-Bis(4-N-isopropylamidinophenyl)-3,4-ethylenedioxythiophene dihydrochloride (6)

Freshly distilled isopropylamine (1 mL, 0.719 g, 12.1 mmol) was added to a stirred suspension of diimidate ester **4** (0.48 g, 1 mmol) in anhydrous methanol (10 mL) and the mixture was stirred for 24 h at RT. The solvent was removed under reduced pressure and methanol saturated with HCl gas (10 mL) was added to the residue. The solution was stirred for 2 h at 40 °C, cooled to RT and precipitated with dry diethyl ether. The yellow solid was filtered off and dried under vacuum at 80 °C for 24 h to yield 0.204 g (37.6%), mp > 250 °C; IR $\nu_{\text{max}}/\text{cm}^{-1}$: 3435, 3157, 1680, 1604, 1435, 1364, 1285, 1080, 854, 767, 555; ^1H NMR ($\text{DMSO}-d_6$) δ/ppm : 9.56 (br s, 2H, NH), 9.42 (br s, 2H, NH), 9.02 (br s, 2H, NH), 7.92 (d, 4H, $J = 8.47$ Hz, ArH), 7.79 (d, 4H, $J = 8.46$ Hz, ArH), 4.51 (s, 4H, $\text{OCH}_2\text{CH}_2\text{O}$), 4.04–4.02 (m, 2H, CH), 1.29 (d, 12H, $J = 6.28$ Hz, CH_3); ^{13}C NMR ($\text{DMSO}-d_6$) δ/ppm : 161.6, 141.2, 136.9, 129.6, 127.5, 125.7, 114.6, 65.3, 45.6, 21.7; HRMS: calcd. for $\text{C}_{26}\text{H}_{31}\text{N}_4\text{O}_2\text{S}$ ($M + 1$)⁺, 463.2168; found: 463.2160. Anal. calcd. for $\text{C}_{26}\text{H}_{30}\text{N}_4\text{O}_2\text{S} \cdot 2\text{HCl} \cdot 3\text{H}_2\text{O}$ ($M_r = 589.58$): C 52.97, H 6.50, N 9.50, S 5.44; found: C 53.33, H 6.14, N 9.29, S 5.10.

4.1.4. 2,5-Bis(4-N-isobutylamidinophenyl)-3,4-ethylenedioxythiophene dihydrochloride (7)

Imidate ester **4** (0.614 g, 1.26 mmol) was suspended in anhydrous methanol (60 mL), isobutylamine (1 mL, 0.736 g, 10 mmol) was added under a nitrogen atmosphere and the mixture was stirred for 18 h at RT. The solvent was removed under reduced pressure and methanol saturated with HCl gas (10 mL) was added

to the residue. The solution was stirred for 4 h at 40 °C, cooled to RT and dry diethyl ether was added. The precipitate was filtered off and dried under vacuum at 80 °C for 24 h to yield 0.312 g (43.4%) of pale yellow powder, mp > 250 °C; IR $\nu_{\text{max}}/\text{cm}^{-1}$: 2972, 1670, 1520, 1319, 1095, 818, 738, 644; ^1H NMR ($\text{DMSO}-d_6$) δ/ppm : 9.87 (s, 2H, NH), 9.52 (s, 2H, NH), 9.13 (s, 2H, NH), 7.92 (d, 4H, $J = 8.60$ Hz, ArH), 7.84 (d, 4H, $J = 8.60$ Hz, ArH), 4.50 (s, 4H, $\text{OCH}_2\text{CH}_2\text{O}$), 3.27 (t, 4H, $J = 6.56$ Hz, NHCH_2CH), 2.03 (m, 2H, $J = 6.78$ Hz, $\text{CH}_2\text{CH}(\text{CH}_3)_2$), 0.98 (d, 12H, $J = 6.66$ Hz, CH_3); ^{13}C NMR ($\text{DMSO}-d_6$) δ/ppm : 162.3, 140.7, 136.51, 129.0, 126.8, 125.3, 114.1, 64.8, 49.5, 27.0, 19.9; HRMS: calcd. for $\text{C}_{28}\text{H}_{35}\text{N}_4\text{O}_2\text{S}$ ($M + 1$)⁺, 491.2481; found: 491.2453. Anal. calcd. for $\text{C}_{28}\text{H}_{34}\text{N}_4\text{O}_2\text{S} \cdot 2\text{HCl} \cdot 2\text{H}_2\text{O}$ ($M_r = 599.62$): C 56.09, H 6.72, N 9.34, S 5.35; found: C 56.38, H 6.33, N 9.52, S 5.31.

4.1.5. 2,5-Bis(4-N-cyclopentylamidinophenyl)-3,4-ethylenedioxythiophene dihydrochloride (8)

To a suspension of compound **4** (0.626 g, 1.28 mmol) in anhydrous methanol (40 mL), under a nitrogen atmosphere, cyclopentylamine (0.296 g, 3.48 mmol) was added and the mixture was stirred for 48 h at RT. The solvent was removed under reduced pressure and methanol saturated with HCl gas (10 mL) was added to the residue. The solution was stirred under reflux for 6 h, then cooled to RT and dry diethyl ether was added. The precipitate was filtered off and dried under vacuum at 80 °C for 24 h to yield 0.245 g (32.6%) of pale yellow powder, mp > 250 °C; IR $\nu_{\text{max}}/\text{cm}^{-1}$: 3042, 2960, 1671, 1608, 1510, 1486, 1443, 1410, 1362, 1085, 843, 747; ^1H NMR ($\text{DMSO}-d_6$) δ/ppm : 9.68 (br s, 2H, NH), 9.48 (br s, 2H, NH), 9.10 (br s, 2H, NH), 7.91 (d, 4H, $J = 8.21$ Hz, ArH), 7.80 (d, 4H, $J = 8.33$ Hz, ArH), 4.50 (s, 4H, $\text{OCH}_2\text{CH}_2\text{O}$), 4.19–4.11 (m, 2H, CH), 2.16–2.09 (m, 4H, CH_2), 1.78–1.57 (m, 12H, CH_2); ^{13}C NMR ($\text{DMSO}-d_6$) δ/ppm : 162.5, 141.2, 136.9, 129.6, 127.5, 125.8, 114.6, 65.3, 54.7, 31.8, 24.1; HRMS: calcd. for $\text{C}_{30}\text{H}_{35}\text{N}_4\text{O}_2\text{S}$ ($M + 1$)⁺, 515.2481; found: 515.2460. Anal. calcd. for $\text{C}_{30}\text{H}_{34}\text{N}_4\text{O}_2\text{S} \cdot 2\text{HCl} \cdot 4.5\text{H}_2\text{O}$ ($M_r = 668.68$): C 53.89, H 6.78, N 8.38, S 4.80; found: C 53.65, H 6.50, N 8.11, S 5.02.

4.1.6. 2,5-Bis[4-(2-imidazolyl)phenyl]-3,4-ethylenedioxythiophene dihydrochloride (9)

A suspension of the imidate ester salt **4** (0.68 g, 1.4 mmol) in 30 mL anhydrous methanol and ethylenediamine (0.192 g, 3.2 mmol) was heated under reflux for 12 h under a nitrogen atmosphere. The solvent was removed under reduced pressure and the residue was washed with diethyl ether, dried and dissolved in dry methanol saturated with HCl(g). The mixture was stirred under reflux for 5 h, the solvent was partially evaporated and dry diethyl ether was added. The resultant solid was filtered off, washed with diethyl ether and dried under vacuum at 80 °C for 24 h to yield 0.325 g (46.2%) of yellow powder, mp > 250 °C; IR $\nu_{\text{max}}/\text{cm}^{-1}$: 3402, 3125, 1615, 1577, 1510, 1365, 1085, 1036, 845, 745, 652; ^1H NMR ($\text{DMSO}-d_6$) δ/ppm : 10.57 (s, 4H, NH_2), 8.03 (d, 4H, $J = 8.40$ Hz, ArH), 7.98 (d, 4H, $J = 8.55$ Hz, ArH), 4.52 (s, 4H, $\text{OCH}_2\text{CH}_2\text{O}$), 4.03 (s, 8H, NCH_2); ^{13}C NMR ($\text{DMSO}-d_6$) δ/ppm : 164.6, 141.8, 138.1, 129.8, 126.2, 120.5, 115.1, 65.3, 44.8; HRMS: calcd. for $\text{C}_{24}\text{H}_{23}\text{N}_4\text{O}_2\text{S}$ ($M + 1$)⁺, 431.1542; found: 431.1536. Anal. calcd. for $\text{C}_{24}\text{H}_{22}\text{N}_4\text{O}_2\text{S} \cdot 2\text{HCl} \cdot 6\text{H}_2\text{O}$ ($M_r = 611.54$): C 47.14, H 5.93, N 9.16, S 5.24; found: C 47.28, H 5.68, N 8.77, S 5.24.

4.1.7. 2,5-Bis[4-(1,4,5,6-tetrahydropyrimidin-2-yl)phenyl]-3,4-ethylenedioxythiophene dihydrochloride (10)

A suspension of the imidate ester salt **4** (0.69 g, 1.4 mmol) in 60 mL anhydrous methanol and 1,3-diaminopropane (0.89 g, 12 mmol) was heated under reflux for 3 h under a nitrogen atmosphere. The solvent was removed under reduced pressure and the residue was washed with diethyl ether, dried and dissolved in dry methanol saturated with HCl(g). The mixture was stirred under

reflux for 2 h, the solvent was partially evaporated and dry diethyl ether was added. The resultant solid was filtered off, washed with diethyl ether and dried under vacuum at 80 °C for 24 h to yield 0.56 g (75.1%) of yellow powder, mp > 250 °C; IR $\nu_{\max}/\text{cm}^{-1}$: 2972, 2038, 1610, 1578, 1452, 1365, 1308, 1086, 840, 744, 665; ^1H NMR (DMSO- d_6) δ/ppm : 10.20 (s, 4H, NH), 7.92 (d, 4H, $J = 8.43$ Hz, ArH), 7.87 (d, 4H, $J = 8.43$ Hz, ArH), 4.50 (s, 4H, OCH₂CH₂O), 3.50 (t, 8H, $J = 5.52$ Hz, N-CH₂CH₂), 1.98 (q, 4H, $J = 5.34$ Hz, N-CH₂CH₂); ^{13}C NMR (D₂O) δ/ppm : 159.3, 140.4, 137.0, 127.1, 126.0, 125.7, 114.9, 64.7, 38.9, 17.6; HRMS: calcd. for C₂₆H₂₇N₄O₂S (M + 1)⁺: 459.1855; found: 459.1837. Anal. calcd. for C₂₆H₂₆N₄O₂S·2HCl·3H₂O ($M_r = 585.55$): C 53.33, H 5.85, N 9.57, S 5.48; found: C 53.52, H 5.79, N 9.54, S 5.37.

4.1.8. 3,4-Ethylenedioxythiophene-2,5-dicarboxanilide (**13**)

3,4-Ethylenedioxythiophene-2,5-dicarboxylic acid (**11**) (2.465 g, 0.0107 mol) was suspended in dry benzene (120 mL), thionyl chloride (12 mL, 19.56 g, 0.164 mol) and 12 drops of DMF were added, and the resulting mixture was heated under reflux for 12 h. The solvent was removed under reduced pressure and the residue was washed with dry benzene. The formed diacid chloride was used in the next step without further purification.

To a suspension of diacid chloride in dry chloroform (100 mL), aniline (4.09 g, 0.044 mol) was added under a nitrogen atmosphere, and the mixture was stirred at RT for 24 h. The solvent was evaporated under reduced pressure and the residue was suspended in water. The formed solid was filtered off and washed with 10% HCl, 10% NaHCO₃ and water, and recrystallized from chloroform to yield 2.98 g (73%) of white powder, mp 240–241 °C; IR $\nu_{\max}/\text{cm}^{-1}$: 3380, 3035, 2955, 1652, 1601, 1544, 1484, 1459, 1434, 1374, 1307, 1290, 1240, 1147, 1089, 878, 752, 685, 617, 576, 491; ^1H NMR (CDCl₃) δ/ppm : 8.53 (s, 2H, NH), 7.62 (d, 4H, $J = 7.67$ Hz, ArH), 7.35 (t, 4H, $J = 8.08$ Hz, ArH), 7.13 (t, 2H, $J = 7.41$ Hz, ArH), 4.59 (s, 4H, OCH₂CH₂O); ^{13}C NMR (CHCl₃): 153.02, 133.46, 132.32, 123.84, 119.33, 114.86, 60.13; MS (m/z): 381.2 (M + 1)⁺; Anal. calcd. for C₂₀H₁₆N₂O₄S·0.25H₂O ($M_r = 384.93$): C 62.41, H 4.32, N 7.28, S 8.33; found: C 62.35, H 4.25, N 7.27, S 7.95.

4.1.9. 3,4-Ethylenedioxythiophene-2,5-bis(*N*-phenylamidine) dihydrochloride (**15**)

3,4-Ethylenedioxythiophene-2,5-dicarboxanilide (**13**) (0.997 g, 2.6 mmol) was suspended in dry chloroform (50 mL) under a nitrogen atmosphere, SOCl₂ (2 mL) and 6 drops of dry DMF were added, and the resulting mixture was heated under reflux for 13 h. The solvent was removed under reduced pressure and the residue was washed with dry benzene. Diimidoyl chloride was then suspended in dry chloroform (50 mL), chilled in an ice bath and dry NH₃ gas was passed through for 4 h. The reaction mixture was stirred at RT for 7 days. The solvent was evaporated under reduced pressure and the residue was suspended in water, made basic to pH 10 with 1M NaOH and the precipitate was filtered off, washed with water and dried. The solid was suspended in anhydrous methanol saturated with HCl gas and stirred at RT for 15 h. The volume of the solvent was reduced under reduced pressure and dry diethyl ether was added. The solid was filtered off, washed with dry diethyl ether and dried under vacuum at 80 °C for 24 h to yield 0.9 g (76.8%) of pale yellow powder, mp > 250 °C; IR $\nu_{\max}/\text{cm}^{-1}$: 3066, 1600, 1481, 1357, 1083, 846, 657; ^1H NMR (DMSO- d_6) δ/ppm : 12.07 (br s, 2H, NH), 9.89 (br s, 2H, NH), 9.36 (br s, 2H, NH), 7.55 (t, 4H, $J = 7.64$ Hz, ArH), 7.45–7.41 (m, 6H, ArH), 4.46 (s, 4H, OCH₂CH₂O); ^{13}C NMR (DMSO- d_6) δ/ppm : 154.59, 144.84, 135.39, 130.37, 128.54, 125.40, 108.06, 65.61; HRMS: calcd. for C₂₀H₁₉N₄O₂S (M + 1)⁺: 379.1229; found: 379.1226. Anal. calcd. for C₂₀H₁₈N₄O₂S·2HCl·3H₂O ($M_r = 505.42$): C 47.53, H 5.19, N 11.09, S 6.34; found: C 47.57, H 5.14, N 11.04, S 6.27.

4.1.10. 3,4-Ethylenedioxythiophene-2,5-dicarboxamide (**16**)

Ammonium hydroxide solution (140 mL) was added dropwise to a stirred solution of diacid chloride **12** (3.52 g, 13.2 mmol) in dichloromethane. The formed solid was filtered off, washed with water and recrystallized from methanol to yield 2.41 g (80.2%) of pale brown powder, mp > 250 °C; IR $\nu_{\max}/\text{cm}^{-1}$: 3426, 3185, 1680, 1615, 1484, 1456, 1412, 1354, 1129, 1092, 857, 777, 678, 568; ^1H NMR (CDCl₃) δ/ppm : 7.72 (s, 2H, NH), 6.81 (s, 2H, NH), 4.35 (s, 4H, OCH₂CH₂O); ^{13}C NMR (DMSO- d_6) δ/ppm : 161.70, 141.04, 116.69, 65.44; MS (m/z): 229.1 (M + 1)⁺.

4.1.11. 3,4-Ethylenedioxythiophene-2,5-dicarbonitrile (**17**)

Dry acetonitrile (110 mL) was cooled in an ice bath and then POCl₃ (1.71 mL) and DMF (1.7 mL) were added. The resulting solution was stirred for 1.5 h in an ice bath and 3,4-ethylenedioxythiophene-2,5-dicarboxamide (0.94 g, 4.1 mmol) was added. Pyridine (5.6 mL) was added after stirring for 2 h at RT and the formed suspension was stirred for an additional 1 h at RT. The reaction mixture was extracted with chloroform and the collected organic layers were washed with 10% HCl, saturated NaCl solution and then with water until neutral reaction. The organic phase was dried at Na₂SO₄, the solvent was removed and the residue was recrystallized from ethanol to yield 0.49 g (62.9%) of white powder, mp 133–134 °C; IR $\nu_{\max}/\text{cm}^{-1}$: 3172, 2964, 2214, 1665, 1607, 1506, 1471, 1454, 1390, 1359, 1262, 1083, 851, 801, 670, 583; ^1H NMR (CDCl₃) δ/ppm : 4.43 (s, 4H); ^{13}C NMR (CDCl₃) δ/ppm : 147.69, 110.45, 91.23, 65.12; MS (m/z): 193.1 (M + 1)⁺. Anal. calcd. for C₈H₄N₂O₂S ($M_r = 192.20$): C 49.99, H 2.10, N 14.58, S 16.68; found: C 49.85, H 2.33, N 14.29, S 16.37.

4.2. Spectroscopic studies

Polynucleotides were purchased as noted: polyA–polyU (Sigma), calf thymus (ct)-DNA (Aldrich). Polynucleotides were dissolved in Na-cacodylate buffer, $I = 0.05$ mol dm⁻³, pH 7.0. Calf thymus ct-DNA was additionally sonicated and filtered through a 0.45 μm filter. Polynucleotide concentration was determined spectroscopically as concentration of phosphates [35].

Electronic absorption spectra were obtained on a Varian Cary 100 Bio spectrometer, CD spectra were collected on a Jasco J-810 spectrometer and fluorescence spectra were recorded on a Varian Cary Eclipse fluorimeter; all in quartz cuvettes (1 cm). Measurements were performed in an aqueous buffer solution (pH 7.0 – Na-cacodylate buffer, $I = 0.05$ mol dm⁻³). Absorbance and fluorescence intensities of the studied compounds were proportional to their concentration under the experimental conditions used. Excitation wavelength of $\lambda_{\text{exc}} > 360$ nm was used in fluorimetric titrations to avoid inner filter effects caused by absorption of excitation light by added polynucleotide. The binding constant (K_s) and [bound compound]/[polynucleotide phosphate] ratio (n) were calculated according to the Scatchard equation by non-linear least-square fitting, giving excellent correlation coefficients (>0.999) for the obtained K_s and n values. Thermal melting curves for ds-polynucleotides and their complexes with the compounds were determined, as previously described, by following the absorption change at 260 nm as a function of temperature [35]. The absorbance of a studied compound was subtracted from every curve, and the absorbance scale was normalized. The obtained T_m values are the midpoints of the transition curves, determined from the maximum of the first derivative or graphically by a tangent method. Given ΔT_m values were calculated subtracting T_m of the free nucleic acid from T_m of the complex. Every ΔT_m value here reported was the average of at least two measurements, the error in ΔT_m is ± 0.5 °C.

For the ethidium bromide (**EB**) displacement assay, ethidium bromide ($c = 5 \times 10^{-6}$ mol dm⁻³) was added (r [EB]/[polynucleotide] = 0.1) to a polynucleotide solution ($c = 5 \times 10^{-5}$

mol dm⁻³) and quenching of the **EB**/polynucleotide complex fluorescence emission ($\lambda_{\text{ex}} = 480 \text{ nm}$, $\lambda_{\text{em}} = 600 \text{ nm}$) was monitored as a function of $c(\mathbf{EB})/c(\text{compound})$. The given IC₅₀ values represent the ratio $c(\mathbf{EB})/c(\text{compound}) = [\text{Int}(\mathbf{EB}/\text{polynucleotide}) - \text{Int}(\mathbf{EB}_{\text{free}})]/2$, where $\text{Int}(\mathbf{EB}/\text{polynucleotide})$ is the fluorescence intensity of **EB**/polynucleotide complex and $\text{Int}(\mathbf{EB}_{\text{free}})$ is the fluorescence intensity of free ethidium bromide before polynucleotide addition.

4.3. Biological experiments

4.3.1. Cell culturing

Human tumour cell lines, breast adenocarcinoma (MCF-7), bronchioalveolar carcinoma (NCI-H358), colon adenocarcinoma (CaCo-2), larynx carcinoma (HEp-2), cervix adenocarcinoma (HeLa), gastric adenocarcinoma (AGS), pancreatic carcinoma (MiaPaCa2), and Madine-Darby canine kidney (MDCK) cells, were cultured in tissue culture flasks and grown as monolayers. MCF-7, NCI-H358 and AGS cells were grown in RPMI 1640 medium (Gibco, EU) supplemented with 10% heat-inactivated fetal bovine serum–FBS (Gibco, EU), 2 mM glutamine, 1 mM sodium pyruvate, HEPES and 100 U/0.1 mg penicillin/streptomycin. CaCo-2, HEp-2, HeLa, MiaPaCa and MDCK cells were cultured in Dulbecco's Modified Eagle Medium – DMEM (Gibco, EU) supplemented with 10% FBS 2 mM glutamine, and 100 U/0.1 mg penicillin/streptomycin. To detach them from the flask surface, cells were trypsinized using a 0.25% trypsin/EDTA solution. Cells were cultured in a humidified atmosphere under the conditions of 37 °C/5% of CO₂ gas in a CO₂ incubator (Shell Lab, Sheldon Manufacturing, USA).

4.3.2. Cytotoxicity evaluation by the MTT assay [44]

Synthesized compounds **5–10** and **15** and Hoechst 33258 were prepared as stock solutions in highly pure water. Working solutions in a concentration range of 10⁻³–10⁻⁶ mol dm⁻³ were prepared prior to testing. Cytotoxic effects of the compounds on tested cell lines were determined by the MTT assay. Cells were seeded in 96 micro well flat bottom plates (Greiner, Austria) at a concentration of 2 × 10⁴ cells/mL and left overnight in the CO₂ incubator allowing them to attach to the plate surface. Growing medium was replaced with compound supplemented or control medium and incubated for 72 h. Fresh medium with 5 mg/mL of MTT was added onto cells and incubated for 4 h at 37 °C. Upon media removal, water insoluble MTT-formazan crystals formed inside the living cells were dissolved in DMSO and the absorbance at 570 nm proportional to the number of living cells was measured on an Elisa Microplate Reader (Stat fax 2100, Pharmacia Biotech, Uppsala, Sweden). All experiments were performed at least three times in triplicates.

The GI₅₀ value, defined as the compound concentration (μM) leading to cellular growth inhibition by 50%, was calculated and used as a parameter to compare cytotoxicity among the compounds.

4.3.3. Intracellular distribution

HeLa and MiaPaCa cells (1 × 10⁵ cells per slide) were seeded on microscopic slides 24 h prior to the experiment. Cells were incubated with compound **7** (10⁻⁴ mol dm⁻³), **8** (10⁻⁴ mol dm⁻³), **9** (5 × 10⁻⁶ mol dm⁻³) and Hoechst 33258 (10⁻⁴ mol dm⁻³) for 30, 60, 90, and 120 min, respectively. In order to assess intracellular distribution of tested chemicals over a specific time range, cells were washed with PBS at a specific time, and analyzed under a fluorescence microscope (Axioskop 2 MOT, Carl Zeiss Jena GmbH, Jena, Germany) with Zeiss filter combinations: BP 450–490 and LP 520. Untreated cells washed with PBS were used as negative controls for the presence of intrinsic cell fluorescence. To confirm cell viability, control cells were treated in a propidium iodide

solution (10⁻⁸ mol dm⁻³) for 5 min, washed with PBS, and entry and intracellular distribution of tested chemicals were analyzed under the microscope.

4.3.4. Cell cycle analysis

For cell cycle analysis, HeLa cells (3 × 10⁵ cells per well) were seeded into 6-well plates (Greiner, Austria). Twenty-four hours later, the tested compound **5** and Hoechst 33285 were added at a concentration of 1 × 10⁻⁶ mol dm⁻³ and 1 × 10⁻⁵ mol dm⁻³, respectively. Cells were harvested at different intervals (24, 48 and 72 h) following drug treatment. Floating and adherent cells were collected separately, then combined, washed with phosphate buffer saline (PBS), fixed with 70% ethanol, and stored at –20 °C. Immediately before the analysis, the cell pellets were washed with PBS and resuspended in 1 μg/mL of propidium iodide and 0.2 μg/μL of RNase A. Stained cells were then analyzed with a Becton Dickinson FACScalibur (Becton Dickinson) flow cytometer (20 000 cells were analyzed). The percentage of cells in each cell cycle phase was determined using the ModFit LT™ software (Verity Software House) based on DNA histograms. Tests were performed in triplicates and repeated at least twice.

Acknowledgments

The authors thank Carl F. Verkoelen, PhD, Erasmus Medical Center Rotterdam, Rotterdam, The Netherlands, for providing MDCK cells, Ruder Bošković Institute, Department of Molecular Medicine, Laboratory for Systematic Biomedicine, for their help with FACS analysis and Igor Bratoš, PLIVA Croatia Ltd., Research & Development, for providing high-resolution mass spectral analyses. The Ministry of Science, Education and Sports of the Republic of Croatia financially supported this work through Grants No: 219-0982914-2176, 219-0982914-2179, 053-0982914-2965 and 098-0982914-2918.

References

- [1] Y. Wang, P. Ji, J. Liu, R.R. Broaddus, F. Xue, W. Zhang, *Mol. Cancer* 8 (8) (2009) 1–13.
- [2] R. Yoshikawa, M. Kusunoki, H. Yanagi, M. Noda, J.-I. Furuyama, T. Yamamura, T. Hashimoto-Tamaoki, *Cancer Res.* 61 (2001) 1029–1037.
- [3] C. Bailly, G. Chessa, C. Carrasco, A. Joubert, J. Mann, W.D. Wilson, S. Neidle, *Nucleic Acids Res.* 31 (2003) 1514–1524.
- [4] R.R. Tidwell, D.W. Boykin, Dicationic DNA minor groove binders as antimicrobial agents. in: M. Demeunynck, C. Bailly, W.D. Wilson (Eds.), *DNA and RNA Binders: From Small Molecules to Drugs*, vol. 2. Wiley-VCH, Weinheim, Germany, 2003, pp. 414–460.
- [5] C.J. Stuckling, *Expert Opin. Ther. Patents* 14 (2004) 1693–1724.
- [6] P.G. Baraldi, A. Bovero, F. Fruttarolo, D. Preti, M.A. Tabrizi, M.G. Pavani, R. Romagnoli, *Med. Res. Rev.* 24 (2004) 475–528.
- [7] B.S. Praveen Reddy, S. Murari Sondhi, J.W. Low, *Pharmacol. Ther.* 84 (1999) 1–111.
- [8] S. Neidle, *Nat. Prod. Rep.* 18 (2001) 291–309.
- [9] W.D. Wilson, B. Nguyen, F.A. Tanius, A. Mathis, J.E. Hall, C.E. Stephens, D.W. Boykin, *Curr. Med. Chem.—Anti-Cancer Agents* 5 (2005) 389–408.
- [10] I. Stolić, K. Mišković, A. Magdaleno, A.M. Silber, I. Piantanida, M. Bajić, Lj. Glavaš-Obrovac, *Bioorg. Med. Chem.* 17 (2009) 2544–2554.
- [11] S. Neidle, L.R. Kelland, O.J. Trent, I.J. Simpson, D.W. Boykin, A. Kumar, W.D. Wilson, *Biorg. Med. Chem.* 7 (1997) 1403–1408.
- [12] A. Lansiaux, L. Dassonneville, M. Facompre, A. Kumar, C.E. Stephens, M. Bajić, F. Tanius, W.D. Wilson, D.W. Boykin, C. Bailly, *J. Med. Chem.* 45 (2002) 1994–2002.
- [13] A. Lansiaux, F. Tanius, Z. Mishal, L. Dassonneville, A. Kumar, C.E. Stephens, Q. Hu, W.D. Wilson, D.W. Boykin, C. Bailly, *Cancer Res.* 62 (2002) 7219–7229.
- [14] J.J. Vanden Eynde, A. Mayence, I.T. Johnson, T.L. Huang, M.S. Collins, S. Rebholz, P.D. Walzer, M.T. Cushion, I.O. Donkor, *Med. Chem. Res.* 14 (2005) 143–157.
- [15] A. Mayence, J.J. Vanden Eynde, F.M. Krogstad, D.J. Krogstad, M.T. Cushion, T.L. Huang, *J. Med. Chem.* 47 (2004) 2700–2705.
- [16] K. Bielawska, S. Wolczynski, A. Bielawska, *Pol. J. Pharmacol.* 53 (2001) 143–147.
- [17] J. Sychala, *Bioorg. Chem.* 36 (2008) 183–189.

- [18] D. Maciejewska, P. Kazmierczak, J. Zabinski, I. Wolska, S. Popis, *Monatsh. Chem.* 137 (2006) 1225–1240.
- [19] M. Kožul, I. Stolić, B. Žinić, M. Bajić, *Croat. Chem. Acta* 78 (2005) 551–555.
- [20] S. Mallena, M.P.H. Lee, C. Bailly, S. Neidle, A. Kumar, D.W. Boykin, W.D. Wilson, *J. Am. Chem. Soc.* 126 (2004) 13659–13669.
- [21] Y. Liu, C.J. Collar, A. Kumar, C.E. Stephens, D.W. Boykin, W.D. Wilson, *J. Phys. Chem. B.* 112 (2008) 11809–11818.
- [22] M. Del Poeta, W.A. Schell, C.C. Dykstra, S. Jones, R.R. Tidwell, A. Czarny, M. Bajic, Ma. Bajic, A. Kumar, D.W. Boykin, J.R. Perfect, *Antimicrob. Agents Chemother.* 42 (1998) 2495–2502.
- [23] J.J. Brendle, A. Outlaw, A. Kumar, D.W. Boykin, D.A. Patrick, R.R. Tidwell, K.A. Werbovetz, *Antimicrob. Agents Chemother.* 46 (2002) 797–807.
- [24] a) R.G. Hicks, M.B. Nodwell, *J. Am. Chem. Soc.* 122 (2000) 6746–6753;
b) P. Bilik, F. Tanius, A. Kumar, W.D. Wilson, D.W. Boykin, P. Colson, C. Houssier, M. Facompré, C. Tardy, C. Bailly, *ChemBioChem* 2 (2001) 559–569.
- [25] M. Coffey, B.R. McKellar, B.A. Reinhardt, T. Nijakowski, W.A. Feld, *Synth. Commun.* 26 (1996) 2205–2212.
- [26] J.D. McGhee, P.H. von Hippel, *J. Mol. Biol.* 103 (1976) 679–684.
- [27] A. Rodger, B. Norden, *Circular Dichroism and Linear Dichroism*. Oxford University Press, New York, 1997.
- [28] N. Berova, K. Nakanishi, R.W. Woody, *Circular Dichroism Principles and Applications*, second ed. Wiley-VCH, New York, 2000.
- [29] M. Eriksson, B. Norden, *Methods Enzymol.* 340 (2001) 68–98 (Table I).
- [30] a) B. Norden, F. Tjerneld, *Biopolymers* 21 (1982) 1713–1734;
b) R. Lyng, A. Rodger, B. Norden, *Biopolymers* 31 (1991) 1709–1720;
c) P.E. Schipper, B. Norden, F. Tjerneld, *Chem. Phys. Lett.* 70 (1980) 17–21.
- [31] M. Munde, M.A. Ismail, R. Arafa, P. Peixoto, C.J. Collar, Y. Liu, L. Hu, H. M-David-Cordonnier, A. Lansiaux, C. Bailly, D.W. Boykin, W.D. Wilson, *J. Am. Chem. Soc.* 129 (2007) 13732–13743.
- [32] C.R. Cantor, P.R. Schimmel, *Biophysical Chemistry*, vol. 3, WH Freeman and Co., San Francisco, 1980.
- [33] M. Zhao, L. Ratmeyer, R.G. Peloquin, S. Yao, A. Kumar, J. Sychala, D.W. Boykin, W.D. Wilson, *Bioorg. Med. Chem.* 3 (1995) 785–794.
- [34] N. Gelus, C. Bailly, F. Hamy, T. Klimkait, W.D. Wilson, D.W. Boykin, *Bioorg. Med. Chem.* 7 (1999) 1086–1096.
- [35] B.S. Palm, I. Piantanida, M. Žinić, H.-J. Schneider, *J. Chem. Soc. Perkin Trans. 2* (2000) 385–392.
- [36] D.A. Hewitt, P.F. Watson, G.C.W. England, *Theriogenology* 49 (1998) 1083–1101.
- [37] B. Novak, J.T. Tyson, B. Gyorffy, A. Csikasz-Nagy, *Nat. Cell Biol.* 9 (2007) 724–728.
- [38] R.S. DiPaola, *Clin. Cancer Res.* 8 (2002) 3512–3519.
- [39] T. Sato, T. Koseki, K. Yamato, K. Saiki, K. Konishi, M. Yoshikawa, I. Ishikawa, T. Nishihara, *Infect. Immun.* 70 (2002) 528–534.
- [40] S.-C. Lin, S.-C. Chuehy, C.-J. Hsiao, T.-K. Li, T.-H. Chen, C.-H. Liao, P.-C. Lyuz, J.-H. Guh, *Neoplasia* 9 (2007) 830–839.
- [41] R. Venkatasubramanian, M.A. Henson, N.S. Forbes, *Theor. Biol.* 253 (2008) 98–117.
- [42] J. Bartek, J. Lukas, *Cancer Cell* 3 (2003) 421–429.
- [43] F.S. Hogan, N.K. Krishnegoweda, M. Mikhailova, M.S. Kahlenberg, *J. Surg. Res.* 143 (2007) 58–65.
- [44] G. Mickisch, S. Fajta, H. Bier, R. Tschada, P. Alken, *Urol. Res.* 19 (1991) 99–103.